DOI: 10.1002/cbic.200800411

Identification of Physiological and Toxic Conformations in Aβ42 Aggregates

Yuichi Masuda,[a] Satoko Uemura,[a] Ryutaro Ohashi,[b] Azusa Nakanishi,[b] K. Takegoshi,[b] Takahiko Shimizu,[c, d] Takuji Shirasawa,[c, e] and Kazuhiro Irie*[a]

Aggregation of the 42-residue amyloid β-protein (Aβ42) plays a crucial role in the pathogenesis of Alzheimer's disease (AD). Despite numerous structural studies on Aβ aggregates, the relationship between tertiary structure and toxicity remains unclear. Our proline scanning and solid-state NMR studies suggested that aggregates both of wild-type Aβ42 and of E22K-Aβ42 (one of the mutants related to cerebral amyloid angiopathy) contain two conformers: a major one with a turn at positions 25 and 26, and a minor one with a turn at positions 22 and 23. To identify the toxic conformer, the derivative Aβ42-lactam(22K–23E), in which the side chains at positions 22 and 23 were covalently linked, was synthesized as a minor conformer surrogate, along with Aβ42-lactam(25K–26E) as a major conformer surrogate. The Aβ42-lactam(22K–23E) showed stronger aggregation, neurotoxicity, radical generation, and oligomerization than wild-type Aβ42, whereas in Aβ42-lactam(25K–26E) were weak. The transition from the physiological conformation with a turn at positions 25 and 26 to the toxic conformation with a turn at positions 22 and 23 might be a key event in the pathogenesis of AD.

Introduction

Alzheimer's disease (AD) is characterized by the progressive accumulation of 40- and 42-mer amyloid β-proteins (Aβ40 and Aβ42),[1] the latter of which shows stronger aggregation tendencies and higher neurotoxicity.[2] Since aggregation of Aβ induces neuronal death, elucidation of the tertiary structure of Aβ aggregates is essential for understanding the mechanism of neurotoxicity and developing new therapeutic agents for AD. Extensive biophysical studies have revealed that the full length and long fragments of Aβ peptides form intermolecular parallel β-sheets in amyloid fibrils.[3–5] In addition to β-sheets, the presence of turn or bend structures was also indicated at positions 24–27 in Aβ40 aggregates,[6] positions 27–30 in ^{35Mox}Aβ42 aggregates,[7] positions 26 and 27 in Aβ42 aggregates,[8] and positions 22–29 in Aβ40 aggregates.[9–11] However, the precise positions of the turn or bend structures in the Aβ aggregates were not elucidated, and the relationship between turn position and neurotoxicity remains unclear.

We focused on turns or bends in the central region of Aβ42 because the mutation sites related to familial Alzheimer's disease (FAD) are concentrated at positions 22 and 23: Arctic (E22G),[12,13] Dutch (E22Q),[14] Italian (E22K),[15] and Iowa (D23N).[16] Here we show by solid-state NMR that aggregates both of the wild type Aβ42 and of E22K-Aβ42 (Italian mutation) contain two conformers, with a turn either at positions 22 and 23 or at 25 and 26. Conformationally restricted analogues of these two conformers clearly revealed that the former is highly aggregative and neurotoxic. The identification of the physiological and toxic conformers explain why the structures of Aβ aggregates proposed by several groups are different from each other and provides unique opportunities for the development of antibodies and inhibitors that are specific for the toxic conformation of Aβ42.

Results

Analysis of the secondary structure of Aβ42 aggregates by systematic replacement with proline

Systematic replacement with proline in peptides is a reliable and rapid method for predicting secondary structure.[17] Proline residues are rarely present in β-sheets, whereas they are easily accommodated in turns or bends. To analyze the secondary structure of Aβ42 aggregates, we estimated the thermodynamic stabilities of the aggregates of proline-substituted Aβ42 by measuring critical concentrations after each monomer and

[a] *Y. Masuda, S. Uemura, Prof. K. Irie*
Division of Food Science and Biotechnology
Graduate School of Agriculture, Kyoto University
Kyoto 606-8502 (Japan)
Fax: (+81) 75-753-6284
E-mail: irie@kais.kyoto-u.ac.jp

[b] *Dr. R. Ohashi, A. Nakanishi, Prof. K. Takegoshi*
Department of Chemistry, Graduate School of Science, Kyoto University
Kyoto 606-8502 (Japan)

[c] *Assoc. Prof. Dr. T. Shimizu, Dr. T. Shirasawa*
Research Team for Molecular Biomarkers
Tokyo Metropolitan Institute of Gerontology
Tokyo 173-0015 (Japan)

[d] *Assoc. Prof. Dr. T. Shimizu*
Applied Biological Chemistry
United Graduate School of Agricultural Science
Tokyo University of Agriculture and Technology
Tokyo 183-8509 (Japan)

[e] *Dr. T. Shirasawa*
Department of Ageing Control Medicine
Juntendo University Graduate School of Medicine
Tokyo 113-0033 (Japan)

Supporting information for this article is available on the WWW under http://dx.doi.org/10.1002/cbic.200800411 or from the author.

 © 2009 Wiley-VCH Verlag GmbH & Co. KGaA, Weinheim

aggregate had established equilibrium (Figure 1 A). Of the central-region mutants, E22P-, D23P-, G25P-, and S26P-Aβ42 formed highly stable aggregates. Because the aggregates of V24P-Aβ42 were not stable, a long single loop around positions 22–26 would not exist. These data suggested that Aβ42 aggregates may contain two turns in the central region: one at positions 22 and 23 and the other at positions 25 and 26.

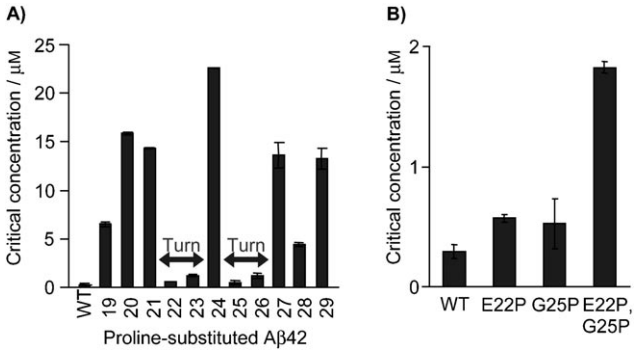

Figure 1. Analysis of secondary structures of Aβ42 aggregates by systematic replacement with proline. A) Thermodynamic stabilities of the Aβ42 aggregates substituted with proline in their central regions. B) Thermodynamic stabilities of the aggregates of the double-proline mutant and single-proline mutants of Aβ42. The molar concentrations of soluble peptides present in equilibrium with aggregates (critical concentrations, *Cr*) were measured after 120 h incubation of each Aβ solution (25 μM) at 37 °C.

To determine whether these two turns could coexist in one Aβ42 molecule, a double mutant (E22P,G25P-Aβ42) was prepared. E22P,G25P-Aβ42 formed significantly less stable aggregates than E22P-Aβ42, G25P-Aβ42, and wild-type Aβ42 (Figure 1 B). This suggests that Aβ42 aggregates contain two different conformers: one with a turn at positions 25 and 26 and the other with a turn at positions 22 and 23. Similar proline scanning by Wetzel's group identified a turn at positions 22 and 23 in Aβ40 aggregates.[18] It is noteworthy that turns at positions 22 and 23 were detected in aggregates both of Aβ42 and Aβ40, and that these positions are the main mutation sites for FAD.

Verification of the presence of two conformers in Aβ42 aggregates by solid-state NMR

To identify the two conformers in Aβ42 aggregates, the tertiary structure at positions 21–27 was analyzed by solid-state NMR. For this purpose, the carbon and nitrogen atoms at these positions in wild-type Aβ42 were labeled with ^{13}C and ^{15}N in multiple patterns (Figure S1 in the Supporting Information). Nitrogen atoms were labeled with ^{15}N to avoid the influence of ^{14}N quadrupole interaction on ^{13}C.[19,20] Since E22K-Aβ42 (Italian), which is related to cerebral amyloid angiopathy (CAA), aggregated more rapidly than wild-type Aβ42,[21] its structure was also analyzed for comparison. Aggregates of the labeled samples were prepared by incubation at 37 °C in phosphate-buffered saline (PBS) under quiescent conditions[9] because of the need to analyze structures under the same conditions as had been employed in other assays to evaluate the activity. The formation of fibrils was confirmed by transmission electron microscopy (Figure S2 in the Supporting Information).

^{13}C,^{1}H dipolar assisted rotational resonance (DARR),[22,23] which allows two-dimensional ^{13}C,^{13}C distance-correlated solid-state NMR spectroscopy, was used to determine the tertiary structures of Aβ42 aggregates. 2D DARR spectra acquired at a mixing time of 20 ms—in which most of the cross-peaks can be ascribed to directly bonded ^{13}C pairs—enabled us to assign all the ^{13}C chemical shifts at positions 21–27 in wild-type Aβ42 and E22K-Aβ42 (Figure 2 A, B, Figures S3–S5 in the Supporting Information, and Tables 1 and 2). Two sets of chemical shifts were observed for Asp23 and Gly25 in both aggregates, indicating that aggregates of wild-type Aβ42 and E22K-Aβ42 contain two conformers quite similar to each other. These were designated as major and minor conformers from the signal intensity of Gly25 in wild-type Aβ42 (Figure 2 C).

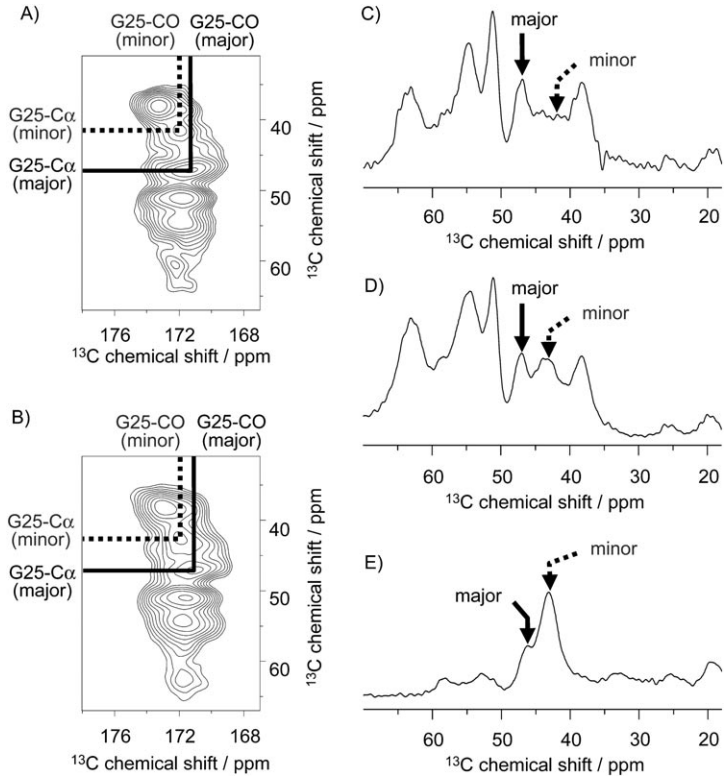

Figure 2. Solid-state NMR structural analysis of aggregates of Aβ42. A), B) 2D DARR spectra (mixing time: 20 ms) of Aβ42 aggregates. Assignment paths of Gly25 are shown. Solid line: major conformer. Dotted line: minor conformer. C)–E) ^{13}C CP-MAS spectra of Aβ42 aggregates. Arrows show signals of C_α in Gly25. Solid arrow: major conformer. Dotted arrow: minor conformer. Samples were wild-type Aβ42 uniformly labeled with ^{13}C and ^{15}N at positions 25–27 (A, C), E22K-Aβ42 uniformly labeled with ^{13}C and ^{15}N at positions 25–27 (B, D), and Aβ42-lactam(22K–23E) in which C_α and C=O in Gly25 were labeled with ^{13}C (E). The ratio of the major and minor conformers was about 1.5:1 for wild-type Aβ42 (C), and about 1.1:1 for E22K-Aβ42 (D). In spectrum E), the peak of the minor conformer with a turn at positions 22 and 23 was almost exclusively observed in aggregates of Aβ42-lactam(22K–23E).

 © 2009 Wiley-VCH Verlag GmbH & Co. KGaA, Weinheim

Table 1. ^{13}C Chemical shifts [δ (ppm)] of wild-type Aβ42 aggregates.[a]

Residue	C=O	C_α	C_β	C_γ	C_δ
Ala21	173.3	48.5	17.9		
	(176.2)[b]	(50.9)	(17.5)		
Glu22	173.4	52.2	32.6	35.1	181.3
	(175.0)	(55.0)	(28.3)	(34.0)	(181.8)
Asp23 (major)[c]	173.3	53.4	36.9	178.6	
Asp23 (minor)	ND[d]	53.4	ND	179.4	
	(174.7)	(52.6)	(39.5)	(178.4)	
Val24	174.4	57.9	32.6	18.3	
	(174.7)	(60.6)	(31.3)	(18.7, 19.5)	
Gly25 (major)	171.2	47.3			
Gly25 (minor)	172.0	41.5			
	(173.3)	(43.5)			
Ser26	171.7	55.5	63.4		
	(173.0)	(56.7)	(62.2)		
Asn27	171.9	51.0	38.3	173.3	
	(173.6)	(51.5)	(37.3)	(175.6)	

[a] TMS was used as an external standard. The uncertainties of all values were within 0.3 ppm. [b] Values in parentheses are chemical shifts in the random coil, adjusted to the TMS reference.[24,25] [c] The ratio of the major and minor conformers was about 1.5:1. CP efficiency did not significantly affect the signal intensity ratio of the two conformers at contact times in the 0.1–0.75 ms range. [d] The ^{13}C chemical shift could not be assigned because of weak signal intensity and/or signal broadening.

Table 2. ^{13}C Chemical shifts [δ (ppm)] of E22K-Aβ42 aggregates.[a,b]

Residue	C=O	C_α	C_β	C_γ	C_δ	C_ε
Ala21	172.9	48.1	18.9			
	(176.2)[c]	(50.9)	(17.5)			
Lys22	173.0	51.7	35.8	24.0	28.6	40.6
	(175.0)	(54.6)	(31.5)	(23.1)	(27.4)	(40.3)
Asp23 (major)[d]	174.5	53.4	40.0	177.7		
Asp23 (minor)	172.7	54.5	38.2	179.1		
	(174.7)	(52.6)	(39.5)	(178.4)		
Val24	174.0	57.4	32.7	18.0, 20.8		
	(174.7)	(60.6)	(31.3)	(18.7, 19.5)		
Gly25 (major)	170.9	47.0				
Gly25 (minor)	172.0	42.5				
	(173.3)	(43.5)				
Ser26	171.8	54.7	63.4			
	(173.0)	(56.7)	(62.2)			
Asn27	171.5	51.0	38.1	173.0		
	(173.6)	(51.5)	(37.3)	(175.6)		

[a] TMS was used as an external standard. The uncertainties of all values were within 0.3 ppm. [b] ^{13}C chemical shifts at positions 21–24 were determined in the previous work.[26] [c] Values in parentheses are chemical shifts in the random coil, adjusted to the TMS reference.[24,25] [d] The ratio of the major and minor conformers was about 1.1:1. In the previous paper[26] we reported the ratio to be about 2.6:1 at Asp23, which was determined roughly from the 1D ^{13}C CP-MAS spectrum. Since the chemical shifts of C_γ at Asp23 of the major and minor conformers are close, it is quite difficult to estimate the ratio accurately. In this paper, the ratio was determined from the chemical shifts of C_α at Gly25, which differ significantly between the major and minor conformers. Moreover, the ratio was determined from the cross-peaks in the 2D DARR spectrum, so the ratio given in this paper should be more precise.

Chemical shifts for $^{13}C_\alpha$ components of amino acid residues are indicators of the secondary structure of peptides; they tend to be more shielded in β-sheets than in α-helices or turns.[24,25] The chemical shifts for $^{13}C_\alpha$ of Gly25 in the minor conformer (δ = 41.5 ppm for wild-type Aβ42, δ = 42.5 ppm for E22K-Aβ42) suggest that each residue is included in a β-sheet (Figure 3 B, D), but those for $^{13}C_\alpha$ of Gly25 in the major conformer (δ = 47.3 ppm for wild-type Aβ42, δ = 47.0 ppm for E22K-Aβ42) suggest that each residue is incorporated in a turn (Figure 3 A, C). We had previously verified the existence of a turn structure at positions 22 and 23 in the minor conformer of E22K-Aβ42 aggregates through a 2D DARR experiment at a mixing time of 500 ms (Figure 3 D).[26] From the similarities in their chemical shifts (Tables 1 and 2), the minor conformer of the wild-type Aβ42 aggregates should also contain a turn structure at positions 22 and 23 (Figure 3 B) similar to that in E22K-Aβ42 (Figure 3 D). These data indicate that the major conformer has a turn at positions 25 and 26 (Figure 3 A, C), and the minor conformer has a turn at positions 22 and 23 (Figure 3 B, D).

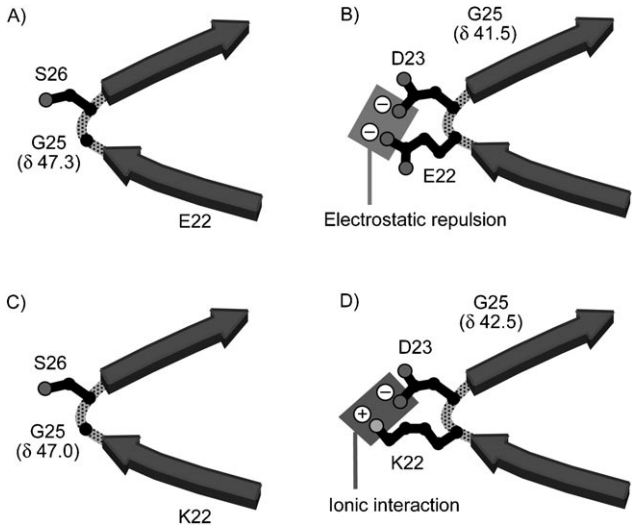

Figure 3. Structural models of the Aβ42 aggregates proposed as a result of systematic replacement with proline and solid-state NMR analyses. A) The major conformer of wild-type Aβ42. B) The minor conformer of wild-type Aβ42. C) The major conformer of E22K-Aβ42. D) The minor conformer of E22K-Aβ42. The structure of (D) was proposed in our previous work.[26] In E22K-Aβ42 (D), an ionic interaction between Lys22 and Asp23 would promote the formation of the turn at this position. On the other hand, the electrostatic repulsion between Glu22 and Asp23 might suppress the formation of the turn at this position in wild-type Aβ42 (B).

It is notable that the amount of the minor conformer in the E22K-Aβ42 aggregates is greater than that in wild-type Aβ42 aggregates (Figures 2 C, D). In E22K-Aβ42 aggregates, an ionic interaction between Lys22 and Asp23 could promote the formation of the turn to increase the ratio of the minor conformer (Figure 3 D). On the other hand, electrostatic repulsion between Glu22 and Asp23 might suppress the formation of the turn in this region to decrease the ratio of the minor conformer in aggregates of wild-type Aβ42 (Figure 3 B). The formation of a salt bridge between Asp23 and Lys28 was reported in wild-type Aβ40 aggregate by Tycko's group[9–11] and in ^{35Mox}Aβ42 aggregate by Riek's group.[7] Quite recently, Teplow and co-workers indicated that the ionic interaction between

 © 2009 Wiley-VCH Verlag GmbH & Co. KGaA, Weinheim

Asp23 and Lys28 could be destabilized by the Italian (E22K) substitution.[27] These data support our speculation with regard to the role of the ionic interaction between Lys22 and Asp23 in the minor conformer of E22K-Aβ42 aggregates, and suggest that Asp23 in the major conformer might interact with Lys28 in a manner similar to that in the structural model proposed by Tycko's group.[9–11] The bend position in Tycko's model of Aβ40 aggregate is at positions 22–29; the center of the bend structure is at positions 25 and 26, which is quite similar to our model of the major conformer of Aβ42 (Figure 3 A, C). In Riek's model of ^{35Mox}Aβ42 aggregate,[7] oxidation of Met35 might shift the bend position of the major conformer (Figure 3 A, C) to positions 27–30.

Identification of the toxic conformation of Aβ42 by use of conformationally restricted analogues

Our solid-state NMR structural analysis suggested that the ionic interaction between Lys22 and Asp23 could increase the proportion of the minor conformer in E22K-Aβ42 (Figure 3 D). In order to evaluate the contribution of each conformer to the aggregation and neurotoxicity of Aβ42, the derivative Aβ42-lactam(22K–23E), in which the side chains of Lys22 and Glu23 were linked with an amide bond, was synthesized as a conformationally restricted analogue of the minor conformer of E22K-Aβ42 (Figure 4 A). Because the distance between the nitrogen and the carbonyl carbon in an amide bond is shorter than that in the above ionic bond, we substituted Asp23 with Glu23 to fill the gap. Aβ42-lactam(25K–26E), in which the side chains of Lys25 and Glu26 were connected with an amide bond, was also prepared as a conformationally restricted analogue of the major conformer of Aβ42 (Figure 4 B). Fixation to the minor conformer of Aβ42-lactam(22K–23E) was confirmed by examining the ^{13}C-1D spectrum of aggregates in which C_α and C=O at Gly25 were labeled with ^{13}C (Figure 2 E).

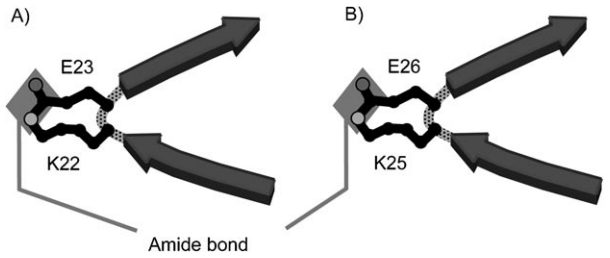

Figure 4. A) The structure of Aβ42-lactam(22K–23E), in which the side chains of Lys22 and Glu23 are linked with an amide bond. B) The structure of Aβ42-lactam(25K–26E), which the side chains of Lys25 and Glu26 are linked with an amide bond. The Aβ42-lactam(22K–23E) and Aβ42-lactam(25K–26E) are conformationally restricted analogues of the minor and major conformer, respectively, in Aβ42 aggregates.

Since the rate of aggregation of Aβ correlates with its neurotoxicity in vitro,[28] the aggregation kinetics of Aβ42 derivatives were estimated by sedimentation assay (Figure 5). The Aβ42-lactam(22K–23E) aggregated far more rapidly than wild-type Aβ42, as did E22K-Aβ42 and E22P-Aβ42. On the other hand, the rate of the aggregation of Aβ42-lactam(25K–26E) was almost identical to that of wild-type Aβ42. The aggregates both of Aβ42-lactam(22K–23E) and of Aβ42-lactam(25K–26E) were as stable as wild-type Aβ42 aggregates (Figure S6 in the Supporting Information). Typical formation of fibrils was confirmed for these Aβ42 derivatives by transmission electron microscopy (Figure 6).

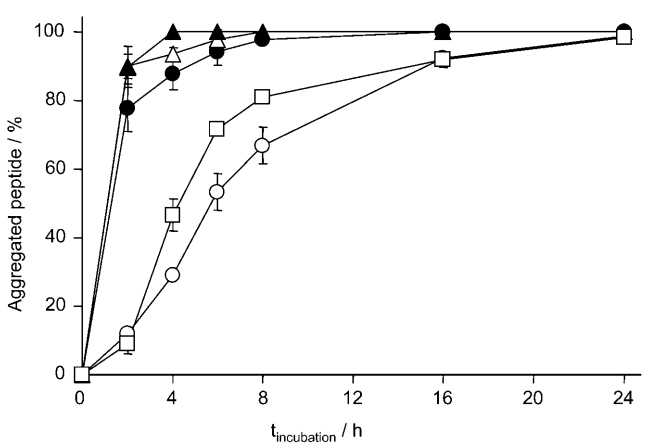

Figure 5. Aggregation kinetics of Aβ derivatives estimated by sedimentation assay with HPLC. ○: Wild-type Aβ42. ●: E22K-Aβ42 (Italian). △: E22P-Aβ42. ▲: Aβ42-lactam(22K–23E). □: Aβ42-lactam(25K–26E).

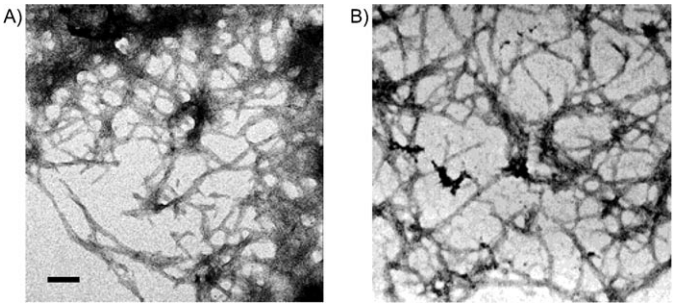

Figure 6. Transmission electron micrographs of negatively stained preparations of fibrils formed by Aβ42 derivatives. Each Aβ peptide (25 μM) was incubated in PBS buffer at 37 °C for 48 h. A) Aβ42-lactam(22K–23E). B) Aβ42-lactam(25K–26E). Scale bar = 100 nm.

The neurotoxicities of these peptides in PC12 cells were estimated by MTT assay; IC_{50} values were calculated by the probit procedure[29] (Table 3). The Aβ42-lactam(22K–23E) (IC_{50}: 0.036 μM) was about four times more neurotoxic than wild-

Table 3. Neurotoxicities of Aβ42 derivatives in PC12 cells as estimated by MTT assay.[a]

Aβ42 derivative	IC_{50} [μM] ± SD
wild-type Aβ42	0.14 ± 0.004
E22K-Aβ42 (Italian)	0.17 ± 0.01
E22P-Aβ42	0.053 ± 0.0006
Aβ42-lactam(22K–23E)	0.036 ± 0.0054
Aβ42-lactam(25K–26E)	1.9 ± 0.61

[a] IC_{50} values were calculated by the probit procedure.[29]

 © 2009 Wiley-VCH Verlag GmbH & Co. KGaA, Weinheim

type Aβ42 (IC_{50}: 0.14 μM). In contrast, the Aβ42-lactam(25K–26E) (IC_{50}: 1.9 μM) was considerably less neurotoxic than wild-type Aβ42. These results suggest that the minor conformer contributes significantly to the neurotoxicity of Aβ42. The major conformer was able to aggregate, but showed only weak neurotoxicity. These findings coincide with our previous data on E22P-Aβ42 and G25P-Aβ42; the former showed more potent aggregative ability and neurotoxicity than wild-type Aβ42, whereas the latter aggregated more slowly and with less neurotoxicity.[28] E22K-Aβ42 was as toxic to PC12 cells as wild-type Aβ42 (Table 3), though E22K-Aβ42 aggregated more rapidly than wild-type Aβ42 (Figure 5). Under the assay conditions with PC12 cells, the ratio of the major and minor conformers might have been almost 1:1, because the minor conformer of E22K-Aβ42 is not fixed, unlike E22P-Aβ42 and Aβ42-lactam-(22K–22E), which showed more potent neurotoxicity than wild-type Aβ42. Alternatively, the potent aggregative ability of E22K-Aβ42 under the assay conditions might have decreased its effective concentration.

The high rate of aggregation and high neurotoxicity of the Aβ42-lactam(22K–23E) might be ascribable to the loss of charge at positions 22 and 23. However, we have previously reported that E22A-Aβ42 and E22V-Aβ42 aggregated far more slowly than wild-type Aβ42 and with less neurotoxicity.[30] This suggests that the strong aggregative ability and neurotoxicity of Aβ42-lactam(22K–23E) should mainly reflect conformational preference rather than the charge effect.

Aβ may induce neurotoxicity through several different pathways.[31] However, the neurotoxicity of Aβ is closely related to oxidative stress, because AD brains display extensive levels of oxidation.[32–34] There is much evidence that Aβ peptides generate free radical species. We estimated the levels of free radicals produced by Aβ42 derivatives by electron spin resonance (ESR) with phenyl-*tert*-butylnitrone (PBN) as a trapping reagent (Figure 7). The Aβ42-lactam(22K–23E) generated more radicals than wild-type Aβ42 and E22P-Aβ42. In contrast, Aβ42-lactam-(25K–26E) produced as many radicals as wild-type Aβ42. These results suggest that a part of the strong neurotoxicity of the minor conformer could be related to its radical-generating activity. However, the radical productivity of Aβ42-lactam(22K–23E) is not significantly stronger than that of E22K-Aβ42. This might be because the neurotoxicity in PC12 cells is affected by other factors such as the affinities of the Aβ peptides to cell membrane.[35,36]

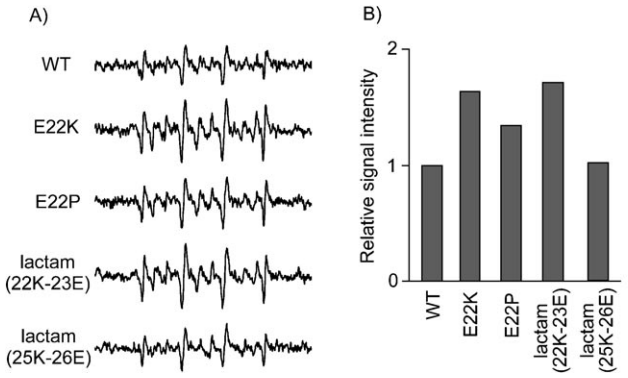

Figure 7. Radical production by Aβ42 derivatives (100 μM) after 48 h incubation at 37 °C measured by ESR with PBN as a spin-trapping reagent. A) ESR spectra after subtraction of the background spectrum (in the presence of PBN without peptides). B) Integral intensities of the ESR signals.

Recent investigations suggest that Aβ oligomers, possible intermediates in the fibril formation process, play a crucial role in the pathogenesis of AD, because they are far more neurotoxic than the monomer and fibrils.[37,38] We anticipated that the formation of the toxic conformation might accelerate the oligomerization of Aβ42. The amount of Aβ42 oligomers was estimated by SDS-PAGE and Western blotting by use of a primary antibody—82E1[39]—that recognizes the N terminus of Aβ (Figure 8). The Aβ42-lactam(22K–23E) formed a substantial amount of soluble oligomers at 1 μM in PBS buffer even immediately after dissolution. E22P-Aβ42, which tends to form a turn at positions 22 and 23, also exhibited the obvious oligomerization. In contrast, Aβ42-lactam(25K–26E) did not form any detectable oligomers. These results suggest that the toxic conformer could trigger the oligomerization of Aβ42. In other words, the tertiary structure of Aβ42 present in oligomers might contain a turn at positions 22 and 23.

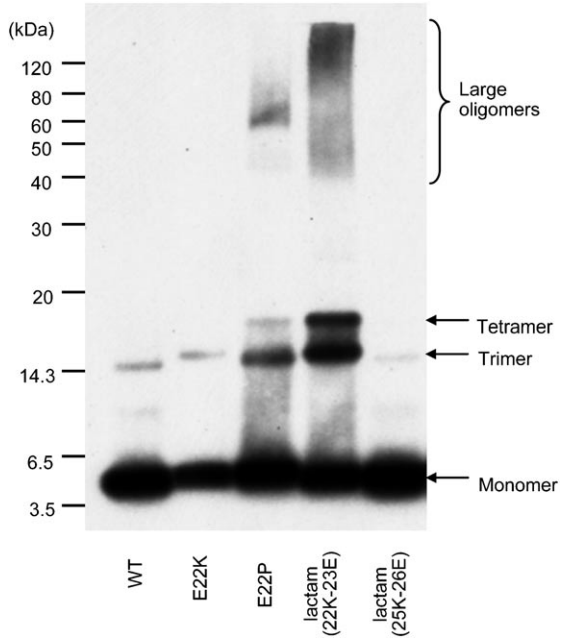

Figure 8. Western blotting of Aβ42 derivatives in PBS buffer immediately after dissolution, separated by SDS-PAGE on a NuPAGE Bis-Tris gel (12%) and probed with the primary antibody 82E1, which recognizes the N terminus of Aβ.

Discussion

From these results, we propose a mechanism for aggregation and neurotoxicity of Aβ42 through conformational change and subsequent formation of radicals (Figure 9). The Aβ42 monomers produced by β- and γ-secretases in membranes would exist in α-helix-rich structures because the Aβ-coding region of APP is embedded in the cell membrane. Shao and co-work-

 © 2009 Wiley-VCH Verlag GmbH & Co. KGaA, Weinheim

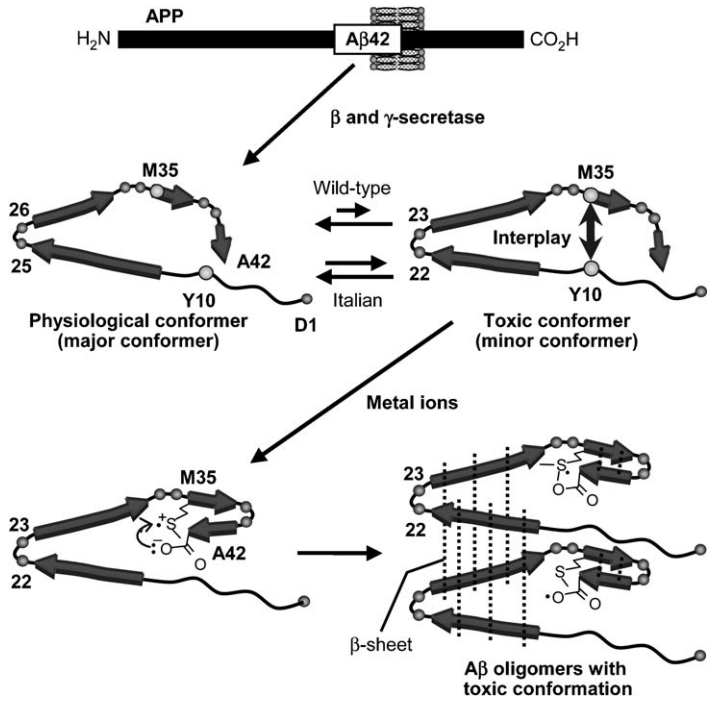

Figure 9. Aggregation of Aβ42 through conformational change and formation of radicals. Aβ42 released from APP by two secretases would adopt a physiological conformer (the major conformer) that is less neurotoxic. Aβ42 could then change its conformation to become toxic (the minor conformer). Formation of a turn structure at positions 22 and 23 would bring the Tyr10 close to Met35 to oxidize the sulfur atom of Met35 in collaboration with metal ions.[43] The resultant S-oxidized radial cation could be stabilized by the C-terminal carboxylate anion to form the C-terminal hydrophobic core that accelerates oligomerization, resulting in long-term oxidative stress.[44,45]

ers[40] reported that Aβ40 and Aβ42 monomers in SDS micelles, which represent conditions similar to cell membranes, form a bend or a loop around positions 25 and 26 located between two α-helices. After release from the cell membrane, Aβ42 monomers could adopt two conformations: a physiological one (major) with a turn at positions 25 and 26 and a toxic one (minor) with a turn at positions 22 and 23. Because Aβ42-lactam(22K–23E) showed far more aggregation and neurotoxicity than Aβ42-lactam(25K–26E), the minor conformer with a turn at positions 22 and 23 should be considered the toxic form.

Many structures of Aβ aggregates in which turns or bends exist around positions 25 and 26 have been reported, as mentioned above.[6–11] We believe these structures might reflect the physiological conformers proposed by us. Although multiple sets of chemical shifts have been observed previously in Aβ40 aggregates,[9] the relationships among them and their relevance to neurotoxicity have not been fully discussed. In this study we have identified two conformers in Aβ42 aggregates and have shown for the first time that the conformer with a turn at positions 22 and 23 is a toxic form. Hoyer and co-workers have recently reported the solution structure of Aβ40 in complexation with the phage-display selected affibody protein $Z_{A\beta3}$, a binding protein of high affinity; this suggests that residues 17–36 comprise a β-hairpin. The center of the bend structure is at positions 25 and 26.[41] This structure might also reflect the physiological conformer before its conformation changes to the toxic one.

It is noteworthy that the mutation sites related to FAD are concentrated at positions 22 and 23 of Aβ.[12–16] We have previously reported that E22Q-Aβ42 (Dutch) and E22K-Aβ42 (Italian), which are related to CAA, aggregated far more rapidly than wild-type Aβ42.[21] Since Lys-Asp and Gln-Asp sequences are frequently found in a turn,[42] these mutants might easily form the toxic conformation with a turn at positions 22 and 23. In this study we have suggested that an ionic interaction between Lys22 and Asp23 in E22K-Aβ42 could promote the formation of the turn at this position to increase the relative proportion of the toxic conformer (Figures 3 and 9). Although Arctic (E22G) and Iowa (D23N) mutations do not lead to CAA, they do cause early onset of AD. This implies that a cause of neurotoxicity of these mutations might be similar to that of Dutch (E22Q) and Italian (E22K).

Radicalization at Tyr10 and Met35 of Aβ42, accompanied by the formation of hydrogen peroxide, plays a critical role in the neurotoxicity.[32–34] In the toxic conformation (Figure 9), the formation of a turn at positions 22 and 23 would bring the Tyr10 close to Met35. In the presence of metal ions, the interplay between these residues[43] could effectively produce the S-oxidized radical cation, the ultimate toxic radical species.[34] Our proline mutagenesis of Aβ42 suggested that the formation of a turn at positions 38 and 39 also enhances aggregation and neurotoxicity.[28] This turn formation could enable the carboxylate anion at the C terminus to stabilize the S-oxidized radical cation through the formation of an intramolecular β-sheet.[44] We have recently verified the existence of the C-terminal intramolecular β-sheet in Aβ42 aggregates by solid-state NMR.[45] The resultant hydrophobic core in the C terminus would accelerate the aggregation of Aβ42 to produce a variety of toxic oligomers. Since such a mechanism is not possible in the C terminus of Aβ40, it could be less neurotoxic than Aβ42.

Barnham's group reported that both Tyr10 and Met35 of Aβ are essential for the reduction of Cu^{II} coordinated with histidine residues (His6, His13, and His14).[46,47] This reaction might be promoted when Aβ42 forms the toxic conformation (Figure 9). The generated Cu^{I} might also induce the production of hydrogen peroxide and the oligomerization of Aβ42 through the formation of a dityrosine crosslink at position 10.[33] The precise mechanism of oligomerization remains to be investigated.

Conclusions

Since proteins and peptides can exist in various conformations, identification of their active conformations is essential for understanding their mechanisms of action. In this study we have identified a physiological conformer with a turn at positions 25 and 26 in Aβ42 aggregates as well as a toxic one with a turn

 © 2009 Wiley-VCH Verlag GmbH & Co. KGaA, Weinheim

at positions 22 and 23. The latter conformer shows potent aggregation and neurotoxicity. Although the toxic conformer might be a minor component, it could play a crucial role in the pathogenesis of AD. Our concept of the toxic conformation clearly explains the mechanism of aggregation and neurotoxicity of Aβ42 through the formation of radicals (Figure 9), and should contribute to the design of antibodies with fewer side effects, as well as to the development of inhibitors that are specific to the toxic conformation of Aβ42.

Experimental Section

General: The following spectroscopic and analytical instruments were used. Peptide synthesizer: Pioneer™ peptide synthesizer (Applied Biosystems, Foster City, CA, USA). HPLC: Waters 600E multisolvent delivery system with a 2487 UV dual λ absorbance detector; Waters 625 LC system with a 486 UV tunable absorbance detector and 741 data module (Milford, MA, USA). Matrix-assisted laser desorption/ionization time-of-flight mass spectrometry (MALDI-TOF-MS): Voyager-DE PRO and 4700 Proteomics Analyzer (Applied Biosystems). Transmission electron microscope: H-7500 electron microscope (Hitachi, Hitachi, Ibaraki, Japan), Solid-state NMR spectrometer: Chemagnetics Infinity NMR spectrometer and Chemagnetics 3.2 mm magic angle spinning (MAS) probe (Chemagnetics/Varian, Palo Alto, CA, USA). Micro plate reader: MultiScan JX (Thermo Scientific, Waltham, MA, USA). ESR: Bruker-EMX PLUS 6/1 spectrometer (Bruker BioSpin K.K., Karlsruhe, Germany). HPLC was carried out on a Develosil-packed column (ODS-UG-5, 20 mm i.d.× 150 mm, 6 mm i.d.×100 mm; Nomura Chemicals, Seto, Japan).

HATU,[48] *N*-α-(9-fluorenylmethoxycarbonyl) (Fmoc) amino acids, Fmoc-Ala-polyethylene glycol-polystylene support (PEG-PS) resin, and *N,N*-diisopropylethylamine (DIPEA) were from Applied Biosystems. *N,N*-Dimethylformamide (DMF), trifluoroacetic acid (TFA), ethane-1,2-dithiol, thioanisole, *m*-cresol, and diethyl ether (peroxide free) were purchased from Nacalai tesque (Kyoto, Japan). Piperidine, 3-(4,5-dimethylthiazol-2-yl)-2,5-diphenyltetrazolium bromide (MTT), Chelex 100 resin, deferoxamine mesylate, and phenyl-*tert*-butylnitrone (PBN) were obtained from Sigma. Micro BCA protein assay kits were purchased from Pierce (Rockford, IL, USA).

Synthesis of Aβ derivatives: The Aβ42 derivatives were synthesized in a stepwise fashion on preloaded Fmoc-Ala-PEG-PS resin (Pioneer™, 0.1 mmol) by the Fmoc method as reported previously.[21,26,28,30,49] The coupling reaction was carried out with the Fmoc amino acid (0.4 mmol), HATU (0.4 mmol), and DIPEA (0.8 mmol) in DMF for 30 min. For the syntheses of Aβ42-lactam(22K–23E) and Aβ42-lactam(25K–26E), Fmoc-Lys-Glu(lactam)-OH was applied to the peptide synthesizer as one Fmoc amino acid. The preparation of Fmoc amino acids labeled with ^{13}C and ^{15}N, and Fmoc-Lys-Glu-(lactam)-OH is described in the Supporting Information. After each coupling reaction, the N-terminal Fmoc group was removed with piperidine in DMF (20%).

After completion of the chain elongation, each peptide resin, washed with DMF and CH_2Cl_2, was treated with a cocktail containing TFA (16 mL), *m*-cresol (0.4 mL), ethanedithiol (1.2 mL), and thioanisole (2.4 mL) for final deprotection and cleavage from the resin. After shaking at room temperature for 2 h, the crude peptide, precipitated by diethyl ether, was purified by HPLC under alkaline conditions as reported previously.[21,26,28,30] Lyophilization gave a corresponding pure Aβ peptide, the purity of which was confirmed by HPLC (>98%). Each purified peptide gave satisfactory mass spectral data on MALDI-TOF-MS (Figures S7–S13 in the Supporting Information). Unlabeled wild-type Aβ42, E22K-Aβ42, and proline-substituted Aβ42 were synthesized by methods reported previously.[21,26,28,30]

Preparation of the aggregates (fibrils) of Aβ42 derivatives labeled with ^{13}C and ^{15}N for solid-state NMR: Each Aβ42 derivative was dissolved in NH_4OH (0.1%) at 250 μM. After a tenfold dilution in sodium phosphate (50 mM) containing NaCl (100 mM) at pH 7.1, the resultant peptide solution (25 μM, pH 7.4) was incubated under quiescent conditions at 37 °C for 48 h. After centrifugation at 21000 *g* and 4 °C, followed by washing with distilled water, the resultant aggregates (fibrils) were dried in vacuo. The weight of the samples was about 11–14 mg.

Transmission electron micrographs of negatively stained preparations of the aggregates (fibrils) formed by Aβ42 derivatives: Fibrillation of the Aβ42 derivatives was confirmed by electron microscope (Figures 6 and S2). Experimental procedures were described elsewhere.[21,26,28]

Solid-state NMR experiments: All solid-state NMR experiments in this study were carried out at 9.4 T (100 MHz for ^{13}C) with a Chemagnetics Infinity NMR spectrometer and Chemagnetics 3.2 mm MAS probe at a spinning frequency of 20 kHz and at room temperature as reported previously.[26] The ^{13}C chemical shifts were calibrated in ppm relative to TMS by taking the ^{13}C chemical shift for the methine ^{13}C of solid adamantane (29.5 ppm) as an external reference standard. For the broadband $^{13}C,^{13}C$ correlation 2D experiment, dipolar-assisted rotational resonance (DARR) was used.[22,23] Pulse sequence parameters of all NMR experiments were: two pulse phase-modulated ^{1}H decoupling power = 120 kHz, variable amplitude cross polarization (VACP) contact time = 0.75 ms, pulse delay = 2 s, t_1 increment = 44 μs, and mixing time (τ) = 20 ms or 500 ms.

Aggregation test: The aggregation kinetics of each Aβ derivative were estimated by sedimentation assay with HPLC as reported previously.[21,28,30] Each Aβ derivative was dissolved in NH_4OH (0.1%) at 250 μM. After a ten-fold dilution in sodium phosphate (50 mM) containing NaCl (100 mM) at pH 7.1, the resultant peptide solution (25 μM, pH7.4) was incubated under quiescent conditions at 37 °C for 2, 4, 6, 8, 16, and 24 h. After centrifugation at 15000 rpm for 10 min at 4 °C, the supernatant (25 μL) was analyzed by HPLC on a Develosil-packed column ODS-UG-5 (6 mm i.d.×100 mm) with elution at 1.0 mL min^{-1} with a 40 min linear gradient of 10–40% CH_3CN/H_2O in 0.1% NH_4OH. The area of absorption at 220 nm was integrated and expressed as a percentage of the control. The thermodynamic stability of each Aβ derivative was estimated from the molar concentration of soluble Aβ peptides present at equilibrium (critical concentration, C_r), which was measured after 120 h incubation by Micro-BCA protein assay.

Estimation of neurotoxicity: Mitochondrial function in rat pheochromocytoma PC12 cells was evaluated by the MTT reduction assay as an indirect measurement of cell viability. We used PC12 cells to estimate the cytotoxicities of the Aβ derivatives. PC12 cells have the potential to differentiate into neural cells, which are sensitive to Aβ peptides, and are generally used for estimating neurotoxicity. The details of the experimental procedure have been described elsewhere.[21,28,30] The colorimetric determination of MTT was made at 595 nm. The absorbance obtained on addition of vehicle was taken as 100%.

ESR spectrometry: The abilities of Aβ42 derivatives to produce radicals were evaluated by ESR with PBN as a spin-trapping reagent in an approach based on Butterfield's protocol[35] with a

 © 2009 Wiley-VCH Verlag GmbH & Co. KGaA, Weinheim

slight modification.[44] PBN was purified by recrystallization from EtOAc/hexane before use. Each Aβ42 derivative was dissolved in NH_4OH (0.1%) at 1 mM. After a ten-fold dilution in sodium phosphate (50 mM) buffer (100 mM NaCl, at pH 7.2) containing PBN (55.6 mM) and deferoxamine mesylate (2.22 mM), the resulting peptide solution (100 μM, 50 mM PBN, 2 mM deferoxamine mesylate) was incubated under quiescent conditions at 37 °C for 48 h. ESR spectrometry was performed with a Bruker-EMX PLUS 6/1 spectrometer at room temperature. To suppress the effect of excess metal-catalyzed reactions, both the ammonium solution and the sodium phosphate buffer were stirred overnight at room temperature in the presence of Chelex-100 resin (50 mg mL^{-1}), followed by filtration with a cellulose acetate syringe filter (0.2 μm, AGC Techno Glass Co. Ltd., Chiba, Japan). The instrument parameters were as follows: sweep width, 100 G; microwave power, 20 mW; microwave frequency, 9.8 GHz; modulation frequency, 100 kHz; modulation amplitude, 1.0 G; conversion time, 40.96 ms; receiver gain, 1×10^5; scans, 100.

Western blot analysis of SDS-PAGE: Gel electrophoresis and Western blotting were performed according to the manufacturer's directions (Invitrogen, Carlsbad, CA). Each Aβ42 derivative was dissolved in NH_4OH (0.1%) at 50 μM. After a 50-fold dilution in sodium phosphate (50 mM) containing NaCl (100 mM) at pH 7.4, the resultant peptide solution (1 μM) was centrifuged at 15000 rpm for 10 min at 4 °C. The supernatant (30 μL) was diluted with lithium dodecyl sulfate sample buffer (Invitrogen, 10 μL). The unheated sample solution (10 μL) was applied to a Bis-Tris NuPAGE gel (12%) and it was electrophoretically separated with morpholinoethanesulfonic acid running buffer (Invitrogen). The peptides were transferred to an Immobilon-P membrane (Millipore, Billerica, MA, USA) and then blocked with Block Ace (Dainippon Sumitomo Seiyaku, Osaka, Japan). The membrane was incubated in the primary antibody 82E1 (Immuno-Biological Laboratories Co., Ltd., Gunma, Japan)[39] at 0.5 μg mL^{-1}, and then in horseradish peroxidase-conjugated anti-mouse IgG (1:1000, Dako, Glostrup, Denmark). Blots were developed by use of enhanced chemiluminescence (ECL, GE Healthcare). Molecular weights were estimated with Low-Range Rainbow Molecular Weight Markers (GE Healthcare) and MagicMark XP Western Standard (Invitrogen).

Acknowledgements

We thank Dr. Naotaka Izumiyama-Shimomura at the Human Tissue Research Group, Tokyo Metropolitan Institute of Gerontology for the use of the electron microscope. This work was supported in part by Grants-in-aid for Scientific Research (A) (Grant No. 18208011 to K.I.), Scientific Research (B) (Grant No. 16380080 to K.I.), Scientific Research on Priority Areas (Grant No. 17025051 to T.S.), and by the Ministry of Education, Culture, Sports, Science and Technology of the Japanese Government with the Promotion of Science for Young Scientists (Grant No. 18.3327 to Y.M.).

Keywords: Alzheimer's disease · amyloid · protein structures · radicals · solid-state NMR

[1] D. J. Selkoe, *Nat. Cell Biol.* **2004**, *6*, 1054–1061.
[2] J. Davis-Salinas, S. M. Saporito-Irwin, C. W. Cotman, W. E. Van Nostrand, *J. Neurochem.* **1995**, *65*, 931–934.
[3] L. C. Serpell, *Biochim. Biophys. Acta, Mol. Basis Dis.* **2000**, *1502*, 16–30.
[4] J. J. Balbach, A. T. Petkova, N. A. Oyler, O. N. Antzutkin, D. J. Gordon, S. C. Meredith, R. Tycko, *Biophys. J.* **2002**, *83*, 1205–1216.
[5] O. N. Antzutkin, R. D. Leapman, J. J. Balbach, R. Tycko, *Biochemistry* **2002**, *41*, 15436–15450.
[6] N. A. Whittemore, R. Mishra, I. Kheterpal, A. D. Williams, R. Wetzel, E. H. Serpersu, *Biochemistry* **2005**, *44*, 4434–4441.
[7] T. Lührs, C. Ritter, M. Adrian, D. Riek-Loher, B. Bohrmann, H. Döbeli, D. Schubert, R. Riek, *Proc. Natl. Acad. Sci. USA* **2005**, *102*, 17342–17347.
[8] A. Olofsson, A. E. Sauer-Eriksson, A. Öhman, *J. Biol. Chem.* **2006**, *281*, 477–483.
[9] A. T. Petkova, R. D. Leapman, Z. Guo, W. M. Yau, M. P. Mattson, R. Tycko, *Science* **2005**, *307*, 262–265.
[10] A. T. Petkova, W. M. Yau, R. Tycko, *Biochemistry* **2006**, *45*, 498–512.
[11] R. Tycko, *Q. Rev. Biophys.* **2006**, *39*, 1–55.
[12] C. Nilsberth, A. Westlind-Danielsson, C. B. Eckman, M. M. Condron, K. Axelman, C. Forsell, C. Stenh, J. Luthman, D. B. Teplow, S. G. Younkin, J. Näslund, L. Lannfelt, *Nat. Neurosci.* **2001**, *4*, 887–893.
[13] K. Kamino, H. T. Orr, H. Payami, E. M. Wijsman, M. E. Alonso, S. M. Pulst, L. Anderson, S. O'Dahl, E. Nemens, J. A. White, A. D. Sadovnick, M. J. Ball, J. Kaye, A. Warren, M. McInnis, S. E. Antonarakis, J. R. Korenberg, V. Sharma, W. Kukull, E. Larson, L. L. Heston, G. M. Martin, T. D. Bird, G. D. Schellenberg, *Am. J. Hum. Genet.* **1992**, *51*, 998–1014.
[14] E. Levy, M. D. Carman, I. J. Fernandez-Madrid, M. D. Power, I. Lieberburg, S. G. van Duinen, G. T. Bots, W. Luyendijk, B. Frangione, *Science* **1990**, *248*, 1124–1126.
[15] F. Tagliavini, G. Rossi, A. Padovani, M. Magoni, G. Andora, M. Sgarzi, A. Bizzi, M. Savoiardo, F. Carella, M. Morbin, G. Giaccone, O. Bugiani, *Alzheimer's Rep.* **1999**, *2*, S28.
[16] T. J. Grabowski, H. S. Cho, J. P. Vonsattel, G. W. Rebeck, S. M. Greenberg, *Ann. Neurol.* **2001**, *49*, 697–705.
[17] S. J. Wood, R. Wetzel, J. D. Martin, M. R. Hurle, *Biochemistry* **1995**, *34*, 724–730.
[18] A. D. Williams, E. Portelius, I. Kheterpal, J. Guo, K. D. Cook, Y. Xu, R. Wetzel, *J. Mol. Biol.* **2004**, *335*, 833–842.
[19] J. G. Hexem, M. H. Frey, S. J. Opella, *J. Am. Chem. Soc.* **1981**, *103*, 224–226.
[20] A. Naito, S. Ganapathy, C. A. McDowell, *J. Chem. Phys.* **1981**, *74*, 5393–5397.
[21] K. Murakami, K. Irie, A. Morimoto, H. Ohigashi, M. Shindo, M. Nagao, T. Shimizu, T. Shirasawa, *J. Biol. Chem.* **2003**, *278*, 46179–46187.
[22] K. Takegoshi, S. Nakamura, T. Terao, *Chem. Phys. Lett.* **2001**, *344*, 631–637.
[23] K. Takegoshi, S. Nakamura, T. Terao, *J. Chem. Phys.* **2003**, *118*, 2325–2341.
[24] D. S. Wishart, B. D. Sykes, *J. Biomol. NMR* **1994**, *4*, 171–180.
[25] D. S. Wishart, C. G. Bigam, A. Holm, R. S. Hodges, B. D. Sykes, *J. Biomol. NMR* **1995**, *5*, 67–81.
[26] Y. Masuda, K. Irie, K. Murakami, H. Ohigashi, R. Ohashi, K. Takegoshi, T. Shimizu, T. Shirasawa, *Bioorg. Med. Chem.* **2005**, *13*, 6803–6809.
[27] M. A. Grant, N. D. Lazo, A. Lomakin, M. M. Condron, H. Arai, G. Yamin, A. C. Rigby, D. B. Teplow, *Proc. Natl. Acad. Sci. USA* **2007**, *104*, 16522–16527.
[28] A. Morimoto, K. Irie, K. Murakami, Y. Masuda, H. Ohigashi, M. Nagao, H. Fukuda, T. Shimizu, T. Shirasawa, *J. Biol. Chem.* **2004**, *279*, 52781–52788.
[29] M. Sakuma, *Appl. Entomol. Zool.* **1998**, *33*, 339–347.
[30] K. Murakami, K. Irie, A. Morimoto, H. Ohigashi, M. Shindo, M. Nagao, T. Shimizu, T. Shirasawa, *Biochem. Biophys. Res. Commun.* **2002**, *294*, 5–10.
[31] D. H. Small, S. S. Mok, J. C. Bornstein, *Nat. Rev. Neurosci.* **2001**, *2*, 595–598.
[32] K. J. Barnham, C. L. Masters, A. I. Bush, *Nat. Rev. Drug Discovery* **2004**, *3*, 205–214.
[33] D. G. Smith, R. Cappai, K. J. Barnham, *Biochim. Biophys. Acta* **2007**, *1768*, 1976–1990.
[34] D. A. Butterfield, A. Castegna, C. M. Lauderback, J. Drake, *Neurobiol. Aging* **2002**, *23*, 655–664.
[35] S. Varadarajan, S. Yatin, M. Aksenova, D. A. Butterfield, *J. Struct. Biol.* **2000**, *130*, 184–208.
[36] G. D. Ciccotosto, D. Tew, C. C. Curtain, D. Smith, D. Carrington, C. L. Masters, A. I. Bush, R. A. Cherny, R. Cappai, K. J. Barnham, *J. Biol. Chem.* **2004**, *279*, 42528–42534.
[37] C. G. Glabe, *Neurobiol. Aging* **2006**, *27*, 570–575.
[38] C. Haass, D. J. Selkoe, *Nat. Rev. Mol. Cell. Biol.* **2007**, *8*, 101–112.

 © 2009 Wiley-VCH Verlag GmbH & Co. KGaA, Weinheim

[39] Y. Horikoshi, G. Sakaguchi, A. G. Becker, A. J. Gray, K. Duff, P. S. Aisen, H. Yamaguchi, M. Maeda, N. Kinoshita, Y. Matsuoka, *Biochem. Biophys. Res. Commun.* **2004**, *319*, 733–737.
[40] H. Shao, S. Jao, K. Ma, M. G. Zagorski, *J. Mol. Biol.* **1999**, *285*, 755–773.
[41] W. Hoyer, C. Grönwall, A. Jonsson, S. Ståhl, T. Härd, *Proc. Natl. Acad. Sci. USA* **2008**, *105*, 5099–5104.
[42] P. Y. Chou, G. D. Fasman, *J. Mol. Biol.* **1977**, *115*, 135–175.
[43] K. Murakami, H. Hara, Y. Masuda, H. Ohigashi, K. Irie, *ChemBioChem* **2007**, *8*, 2308–2314.
[44] K. Murakami, K. Irie, H. Ohigashi, H. Hara, M. Nagao, T. Shimizu, T. Shirasawa, *J. Am. Chem. Soc.* **2005**, *127*, 15168–15174.
[45] Y. Masuda, S. Uemura, A. Nakanishi, R. Ohashi, K. Takegoshi, T. Shimizu, T. Shirasawa, K. Irie, *Bioorg. Med. Chem. Lett.* **2008**, *18*, 3206–3210.
[46] K. J. Barnham, F. Haeffner, G. D. Ciccotosto, C. C. Curtain, D. Tew, C. Mavros, K. Beyreuther, D. Carrington, C. L. Masters, R. A. Cherny, R. Cappai, A. I. Bush, *FASEB J.* **2004**, *18*, 1427–1429.
[47] F. E. Ali, F. Separovic, C. J. Barrow, R. A. Cherny, F. Fraser, A. I. Bush, C. L. Masters, K. J. Barnham, *J. Pept. Sci.* **2005**, *11*, 353–360.
[48] L. A. Carpino, *J. Am. Chem. Soc.* **1993**, *115*, 4397–4398.
[49] K. Irie, K. Oie, A. Nakahara, Y. Yanai, H. Ohigashi, P. A. Wender, H. Fukuda, H. Konishi, U. Kikkawa, *J. Am. Chem. Soc.* **1998**, *120*, 9159–9167.

Received: June 18, 2008
Published online on December 29, 2008

 © 2009 Wiley-VCH Verlag GmbH & Co. KGaA, Weinheim